Seasonal & Interhemispheric Comparisons of Geocoronal Hα Observations & Forward Modeled WACCM-X & NRLMSISE-00 Simulations

L. T. Ashworth[1] (ashwortl@my.erau.edu), E. J. Mierkiewicz[1], S. M. Nossal[2], L. Qian[3], J. M. McInerney[3], L. M. Haffner[1], & R. C. Woodward[2]

[1]Embry-Riddle Aeronautical University, Daytona Beach, FL; [2]University of Wisconsin-Madison, Madison, WI; [3]NSF National Center for Atmospheric Research, Boulder, CO

EMBRY-RIDDLE Aeronautical University

NCAR Operated by UCAR

Introduction

From 2000-2001, ground-based geocoronal hydrogen Balmer-α (Hα) observations were obtained from Pine Bluff Observatory (PBO) in Wisconsin (43.07°N, 270.33°E) using a high spectral resolution (R ≈ 80,000) Fabry-Perot interferometer (FPI). Bishop et al. (2004) compared the PBO March 2000 observations to forward modeled MSISE-90 Hα intensities using the radiative transport code, lyao_rt (Bishop, 1999). Results indicate that hydrogen column abundances exceed those predicted by MSISE-90. Furthermore, Gallant et al. (2019) compared the PBO 2000-2001 observations to NRLMSISE-00 (MSIS-00) Hα intensities generated by lyao_rt. It was found that the observed dusk-to-dawn intensity variation and MSIS-00 show good agreement near the equinoxes and summer solstice, however, MSIS-00 underestimates the dusk-to-dawn asymmetry near the winter solstice (Gallant et al., 2019). More recent work has focused on forward modeling Whole Atmosphere Community Climate Model-eXtended (WACCM-X) simulations for three separate observatory locations, including PBO, Kitt Peak National Observatory (KPNO) in Arizona (31.98°N, 111.60°W), and Cerro Tololo Inter-American Observatory (CTIO) in Chile (30.17°S, 70.80°W). In this study, we focus on comparing PBO WACCM-X forward modeled simulations for the equinoxes and solstices to MSIS-00 and the PBO FPI observations. These comparisons are qualitative as the WACCM-X simulations are not fully representative of the observations and were run for the years 2001-2005, perpetual solar maximum conditions, and UT = 0. We also compare the PBO, KPNO, and CTIO WACCM-X simulations for the same conditions to conduct an interhemispheric comparison. Overall, this work aims to contribute to validating hydrogen variability within the WACCM-X numerical model.

Data Description

- Dual etalon FPI with a resolving power of R ≈ 80,000 at Hα and a spectral resolution of ~0.08 Å.
- Series of 20 observing runs between 2000 and 2001 taken at PBO (43.07°N, 270.33°E).
- Solar conditions ($F_{10.7}$ index) vary between 122 and 277 (average 181).
- Geomagnetic conditions (Ap index) vary between 2 and 82 (average 13).
- Each data set includes multiple nights of observations within a two-week period centered around the new Moon.

See Mierkiewicz et al. (2012) for more details.

- **In this work, evening PBO FPI observations near the equinoxes and solstices are compared to PBO WACCM-X forward modeled results (see Figure 1).**

Model Description

	WACCM-X	MSIS-00
Location	PBO, KPNO, CTIO	PBO, KPNO, CTIO
Year(s)	2001-2005	2000
Day of Year	79, 172, 265, 355*	79, 172, 265, 355
Hour	UT 0	UT 0
Kp Index	3	N/A
Ap Index	N/A	15
$F_{10.7}$ Index	200	200

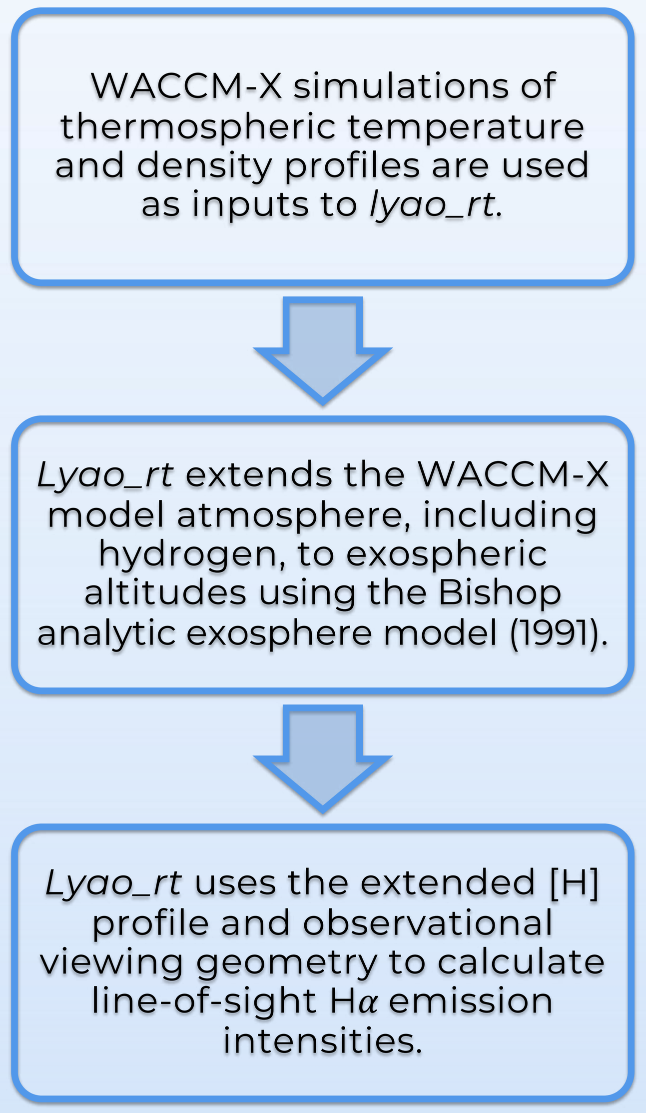

Table 1: WACCM-X and *lyao_rt* inputs used to obtain WACCM-X and MSIS-00 forward modeled intensities. (*) denotes the day of year used for every year except 2004 (leap year). **Chart 1:** The *lyao_rt* process begins with temperature and density profiles from WACCM-X/MSIS-00 and results in calculated forward modeled intensities.

PBO Seasonal Comparison

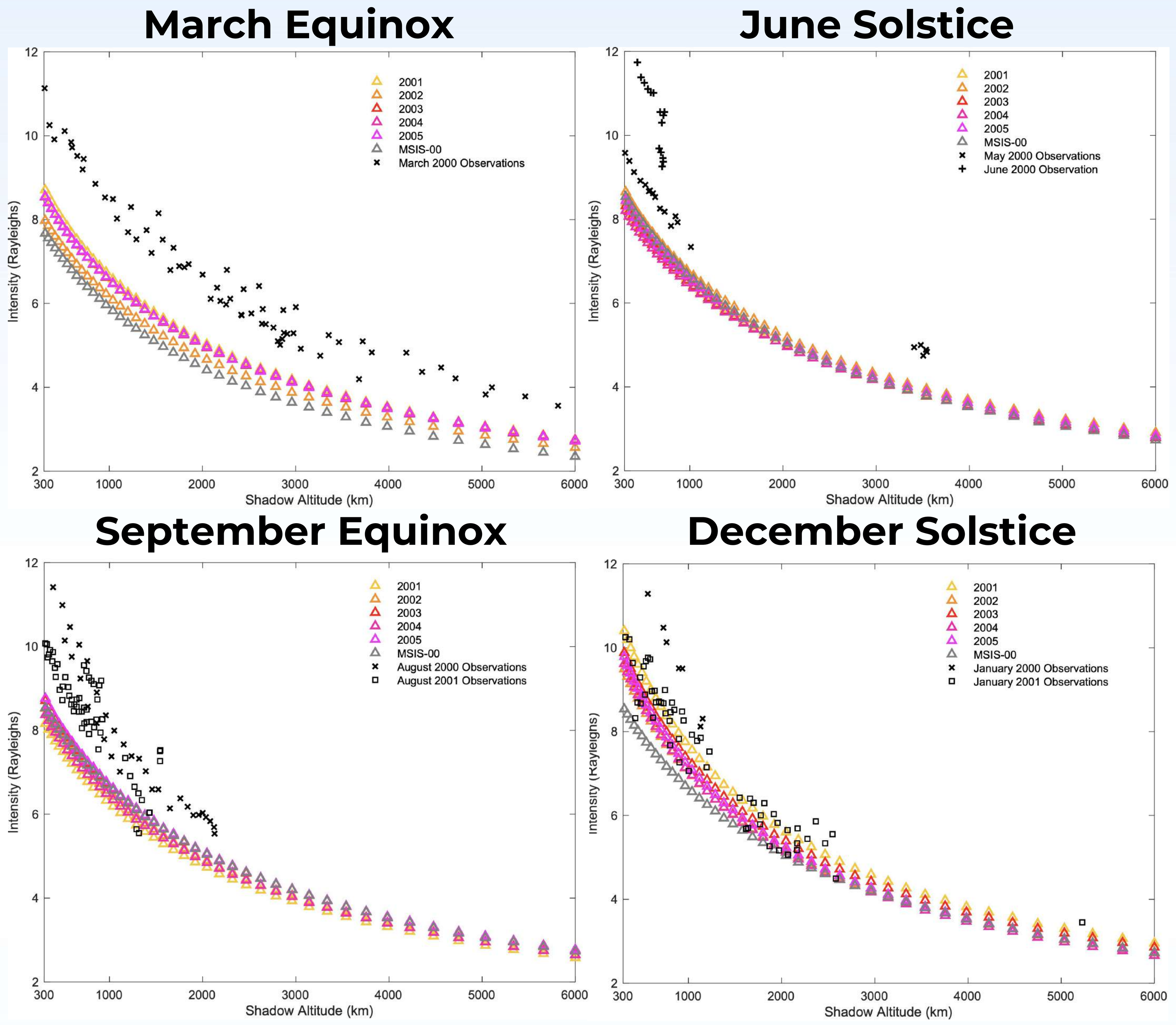

Figure 1: Pine Bluff Observatory (PBO), Wisconsin forward modeled WACCM-X Hα intensities compared to select 2000-2001 PBO FPI observations and a forward modeled MSIS-00 simulation for the **(Top Left)** March equinox, **(Top Right)** June solstice, **(Bottom Left)** September equinox, and **(Bottom Right)** December solstice. Synthetic line-of-sight viewing geometry for the zenith look direction is used here. The observations are not adjusted to account for estimates of tropospheric scattering and the model runs do not account for cascade enhancements.

PBO March Equinox Case Study

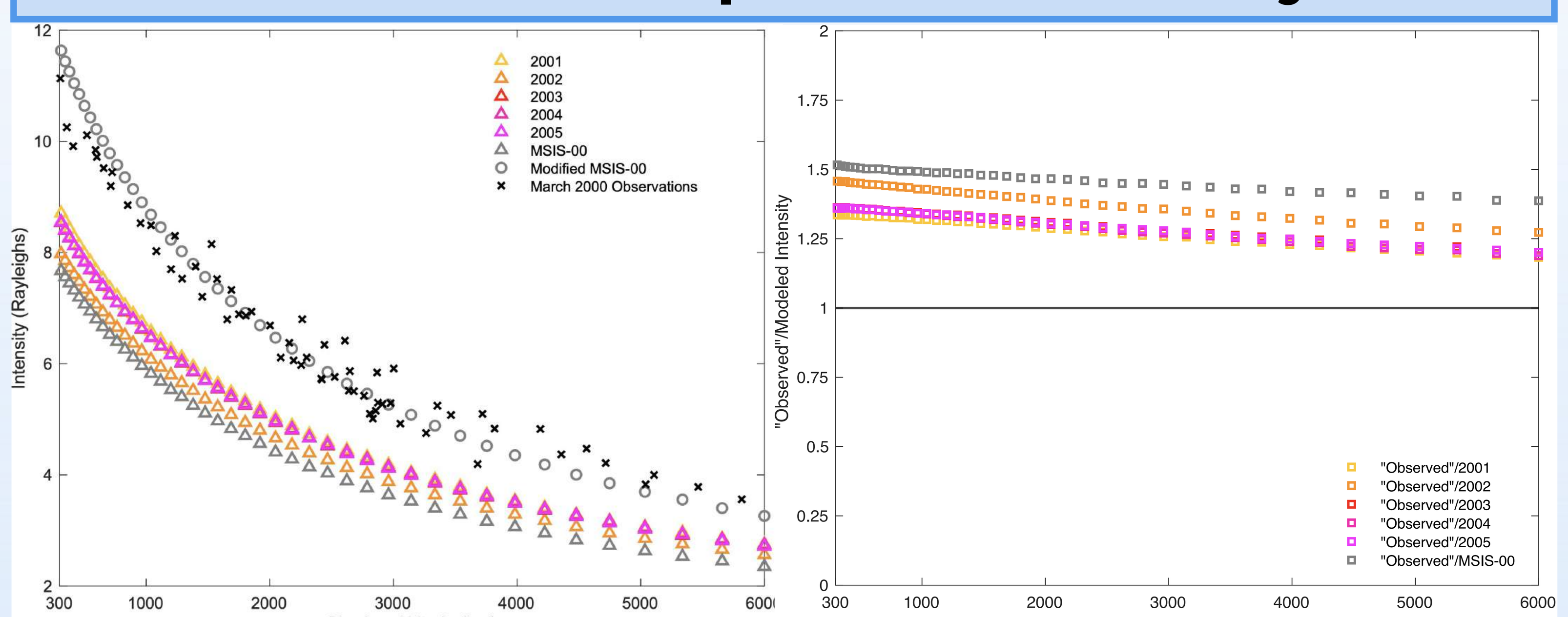

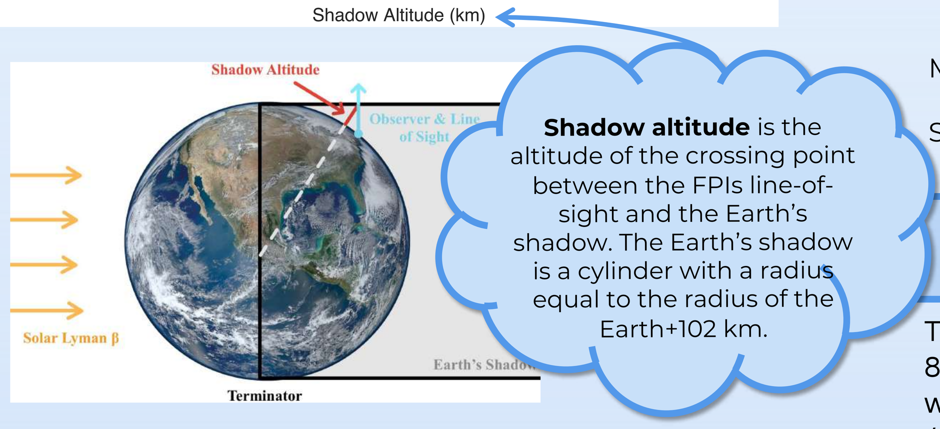

Figure 2: (Left) Same as top left of Figure 1 but now compared to a forward modeled "modified" MSIS-00 simulation. The hydrogen density profile used by lyao_rt to create the modified MSIS-00 intensity profile is based on user-inputted values of exobase density, photochemical upward flux, and mesospheric peak density. Lyao_rt then uses this hydrogen density profile to calculate Hα emission intensity. **(Right)** The modified MSIS-00 intensity profile ("observed") is treated as a proxy to the observations. Here, the ratio of the "observed" to each WACCM-X modeled intensity and the ratio of the "observed" to MSIS-00 modeled intensity is presented. The slope of "observed"/MSIS-00 is flatter than that of the slopes between the "observed" and each WACCM-X simulation.

Interhemispheric Comparison

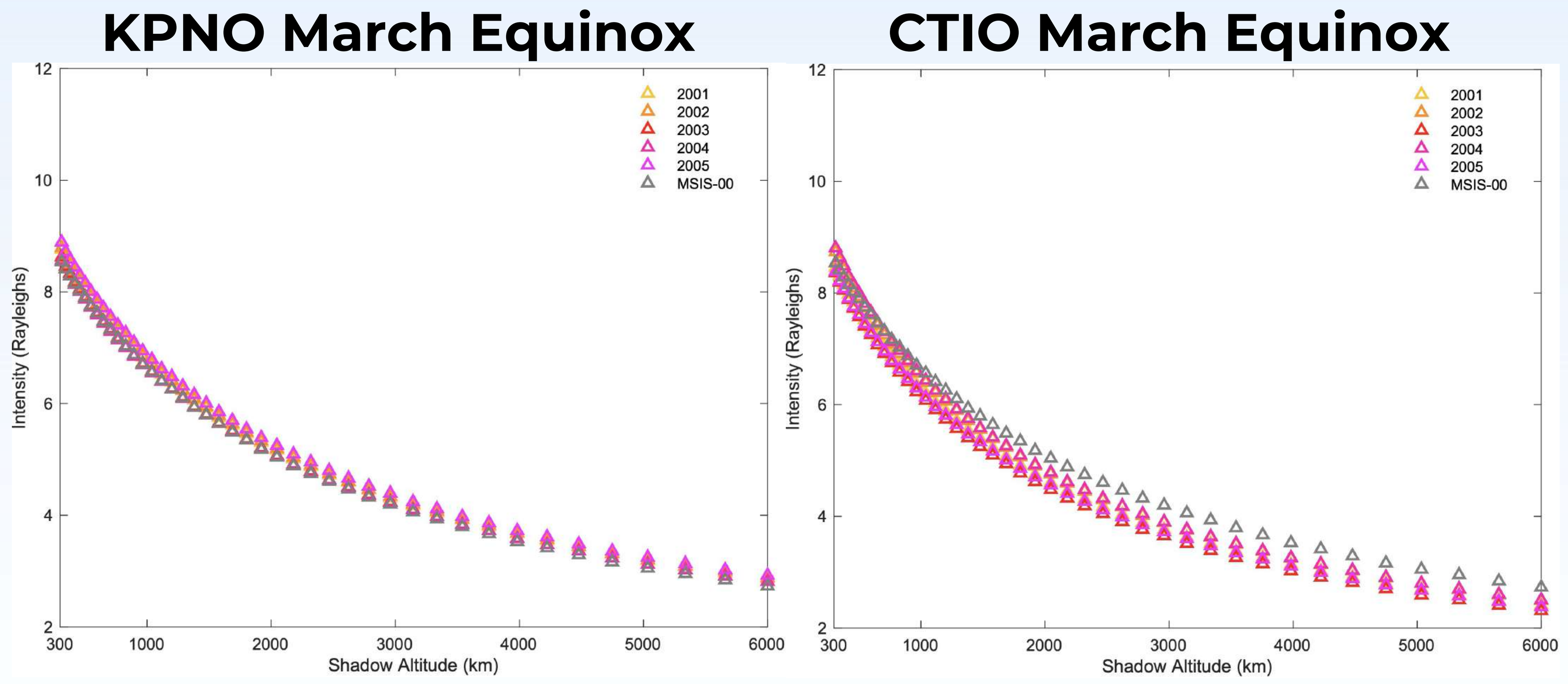

Figure 3: (Left) Kitt Peak National Observatory (KPNO), Arizona and **(Right)** Cerro Tololo Inter-American Observatory (CTIO), Chile forward modeled WACCM-X and MSIS-00 Hα intensities for the March equinox. Synthetic line-of-sight viewing geometry for the zenith look direction is used here.

Conclusions

- WACCM-X shows interannual variability in the hydrogen distribution, which leads to forward modeled intensity variations particularly at lower shadow altitudes (see Figure 1).
- The modified MSIS-00 Hα emission intensity offers better agreement with the March 2000 observations than WACCM-X and MSIS-00 (see Figure 2 and caption).
- WACCM-X offers better agreement in terms of magnitude with the March 2000 PBO FPI observations whereas MSIS-00 offers slightly better agreement with the relative change in intensity with respect to shadow altitude (see Figure 2).
- During the March equinox, KPNO exhibits the highest WACCM-X generated intensity (year 2005) and the least year-to-year variation whereas PBO exhibits the lowest WACCM-X generated intensity (year 2002) and the most year-to-year variation (see Figures 1 & 3).

Future Work

- Use correct line-of-sight viewing geometry as opposed to the synthetic viewing geometry used here.
- Modify MSIS-00 simulations to be used as a proxy to the observations for the June solstice, September equinox, and December solstice.
- Compare WACCM-X simulations for conditions representative of the 2000-2001 PBO and other FPI observations, including correct dates and solar conditions.
- Compare Wisconsin H-Alpha Mapper FPI observations from CTIO and KPNO to forward modeled simulations.

References

Bishop, J. (1991). Analytic exosphere models for geocoronal applications. *Planetary and Space Science* 39, 885–893. doi:10.1016/0032-0633(91)90093-P

Bishop, J. (1999). Transport of Resonant Atomic Hydrogen Emissions in the Thermosphere and Geocorona: Model Description and Applications. *J. Quant. Spectrosc. Radiat. Transfer*, 61, 4, 473—491.

Bishop, J., E. J. Mierkiewicz, F. L. Roesler, J. F. Gomez, and C. Morales (2004), Data-model comparison search analysis of coincident PBO Balmer a, EURD Lyman b geocoronal measurements from March 2000, J. Geophys. Res., 109, A05307, doi:10.1029/2003JA010165.

Gallant, M. A., Mierkiewicz, E. J., Nossal, S. M., Qian, L., Burns, A. G., Zacharias, A. R., & Roesler, F. L. (2019). Signatures of Thermospheric-Exospheric Coupling of Hydrogen in Observed Seasonal Trends of H α Intensity. *Journal of Geophysical Research. Space Physics*, 124(6), 4525–4538. doi:10.1029/2018JA026426.

Mierkiewicz, E. J., F. L. Roesler, and S. M. Nossal (2012). Observed seasonal variations in exospheric effective temperatures. *J. Geophys. Res*, 117, A06313. doi:10.1029/2011JA017123.

Solomon, S. C., Liu, H.-L., Marsh, D. R., McInerney, J. M., Qian, L., & Vitt, F. M. (2019). Whole atmosphere climate change: Dependence of solar activity . *J. Geophys. Res*, 124. doi:10.1029/2019JA026678.

Acknowledgments

This work is supported by NSF CEDAR award 2050077, NSF Astronomy 2009276, and NASA HTMS 80NSSC20K1278, a collaborative effort between ERAU, UW-Madison, UC-Boulder, and NSF NCAR. The authors would like to give a special thanks to the late James Bishop for the development, implementation, and use of the *lyao_rt* code. Additional thanks to Joe McInerney for the WACCM-X simulations used in this study.